

Supplementary Information

Mechanically induced single-molecule white-light emission of excited-state intramolecular proton transfer (ESIPT) materials

*Quan Huang,^a Qiang Guo,^b Jingbo Lan,^{*a} Rongchuan Su,^a You Ran,^a Yudong Yang,^a
Zhengyang Bin^a and Jingsong You^{*a}*

*^aKey Laboratory of Green Chemistry and Technology of Ministry of Education, College of Chemistry,
Sichuan University, 29 Wangjiang Road, Chengdu 610064, People's Republic of China. E-mail:
jingbolan@scu.edu.cn; jsyou@scu.edu.cn*

*^bCollege of Optoelectronic Engineering, Chengdu University of Information Technology, 24 Xuefu Road,
Chengdu 610225, People's Republic of China*

Table of contents

I. General remarks	S3
II. Synthesis of 2-(2-hydroxyphenyl)azole derivatives	S4
III. Steady-state and time-resolved photophysical properties of 6a and 6b	S8
IV. Kinetic derivation and calculation of reversible ESIPT reaction	S16
V. Characterization of mechanochromism	S20
VI. TGA curves of 6a and 6b	S25
VII. Crystal data	S26
VIII. Theoretical calculation	S28
IX. Characterization data of products	S32
X. References	S37
XI. Copies of ^1H and ^{13}C NMR Spectra	S38

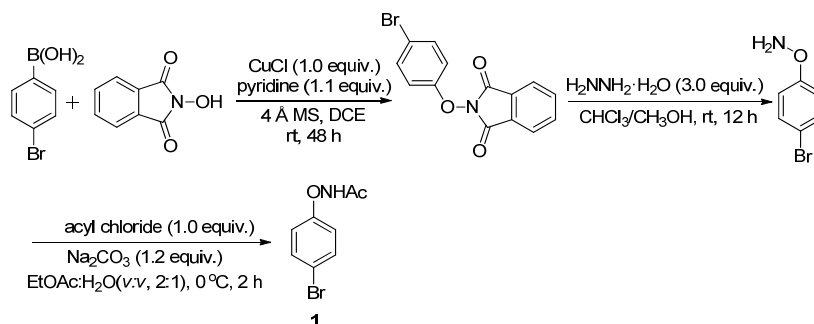
I. General remarks

Unless otherwise noted, all reagents were obtained from commercial suppliers and used without further purification. Solvents were dried and purified using an Innovative Technology PS-MD-5 Solvent Purification System. NMR spectra were obtained on a Varian Inova 400 spectrometer. ^1H NMR (400 MHz) chemical shifts were measured relative to CDCl_3 as the internal reference (CDCl_3 : $\delta = 7.26$ ppm). ^{13}C NMR (100 MHz) chemical shifts were given using CDCl_3 as the internal standard (CDCl_3 : $\delta = 77.16$ ppm). High-resolution mass spectra (HRMS) were obtained with a Shimadzu LCMS-IT-TOF (ESI). X-Ray single-crystal diffraction data were collected on an Agilent Technologies Gemini plus single crystal diffraction. Steady-state UV-visible absorption spectra, fluorescence spectra, excitation spectra and photoluminescence quantum yield were collected on a Horiba Jobin Yvon-Edison Fluoromax-3 fluorescence spectrometer with a calibrated integrating sphere system. To reduce the fluctuation in the excitation intensity, the lamp was kept on for 1 hour prior to the experiment. Powder X-ray diffraction (PXRD) patterns were taken by using X'Pert Pro MPD X-ray diffractometer with a $\text{Cu-K}\alpha$ radiation source ($\lambda = 1.54056 \text{ \AA}$, 40 KV, 35 mA). Thermogravimetric analysis (TGA) was carried out using DTG-60(H) at a rate of $10 \text{ }^\circ\text{C}/\text{min}$ under an N_2 atmosphere. Differential scanning calorimetry (DSC) thermograms were recorded on DSC 200PC equipment under an N_2 atmosphere at a rate of $5 \text{ }^\circ\text{C}/\text{min}$. The nanosecond time-resolved measurements were carried out by a time-correlated single photon counting controller (FluoroHub and Horiba TBX Picosecond Photon Detection, Horiba) with the excitation light source from second harmonic generation of 370 nm of pulse-selected tsunami picosecond laser pulses at 740 nm (Spectra-Physics). Data were fitted with the sum of exponential functions using a nonlinear least-squares procedure in combination with a convolution method. Ultrafast fluorescence up-conversion decay curves were obtained using Time-Tech Spectra UF100 at 350 nm. The femtosecond time-resolved data were fitted to the sum of exponential functions convoluted with the instrument response function, which is fitted to 150 fs determined by the Raman scattering signal.

The IR measurements were conducted on a IRTracer-100 infrared spectrometer using KBr plates. The dichloromethane solution of **6b** was dropped onto the KBr plate, after the solvent volatilized, the IR measurement of pristine **6b** was carried out. The IR measurement of ground **6b** was performed with the powder of ground **6b** fixed by two KBr plates, and the IR measurements of yellowish-green-emitting single crystals and white-emitting single crystals of **6b** were conducted with paraffin wax as adhesive.

II. Synthesis of 2-(2-hydroxyphenyl)azole derivatives

2.1 Synthesis of *N*-(4-bromophenoxy)acetamide (**1**)¹



Scheme S1. Synthetic route of compound **1**.

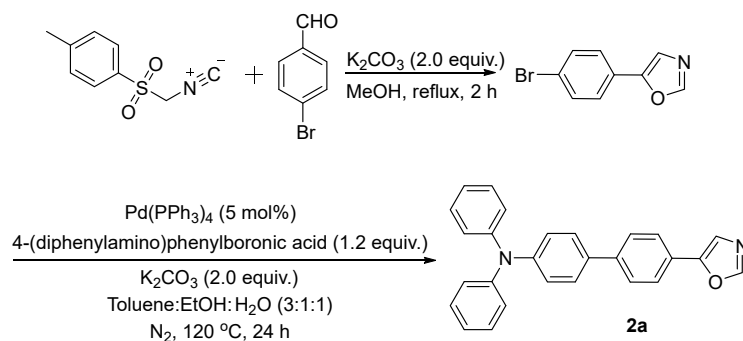
N-(4-Bromophenoxy)acetamide was prepared according to the literature procedures¹. A mixture of *N*-hydroxyphthalimide (815 mg, 5.0 mmol), 4-bromophenylboronic acid (2.01g, 10.0 mmol) and activated 4Å molecular sieves (1.25 g) in 1,2-dichloroethane (DCE, 25.0 mL) were stirred, and then CuCl (495 mg, 5.0 mmol) and pyridine (0.44 mL, 5.5 mmol) were added at room temperature. After the mixture turns green, the filtrate was obtained by filtering and washing with dichloromethane. The solvent was removed under reduced pressure and then the residue was purified by column chromatography on silica gel using petroleum ether/EtOAc (*v/v*) = 5:1 as eluent to provide the desired 2-(4-bromophenoxy)isoindoline-1,3-dione (1.07 g, 67%).

2-(4-Bromophenoxy)isoindoline-1,3-dione (1.07 g, 3.4 mmol, 1.0 equiv.) was dissolved in CHCl₃ (34.0 mL) with 10% MeOH, and stirred at room temperature, followed by adding hydrazine monohydrate (3.0 equiv.). After 12 h, the precipitate was filtered off and washed with dichloromethane. The solvent was then removed

under reduced pressure. The crude product was used without further purification.

The crude product was added to a biphasic mixture of Na_2CO_3 (540 mg, 1.5 equiv.) in a 2:1 mixture of EtOAc:H₂O (6 mL). The resulting solution was cooled to 0 °C, followed by dropwise addition of acyl chloride (1.2 equiv.). After stirring at 0 °C for 2 h, the reaction was quenched with sat. NaHCO_3 and diluted with EtOAc. The organic phase was washed twice with sat. NaHCO_3 , dried over Na_2SO_4 , filtered, and evaporated under reduced pressure. The residue was purified by flash column chromatography on silica gel (dichloromethane/EtOAc = 3/1, v/v) to provide the product (633 mg, 81%).

2.2 Synthesis of 4'-(oxazol-5-yl)-*N,N*-diphenyl-[1,1'-biphenyl]-4-amine (2a)



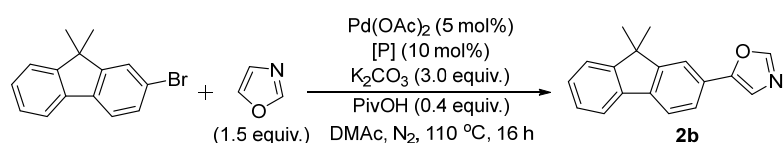
Scheme S2. Synthetic route to compound **2a**.

A mixture of 4-bromobenzaldehyde (1.85 g, 10.0 mmol), tosylmethyl isocyanide (1.95 g, 10.0 mmol) and potassium carbonate (2.76 g, 20.0 mmol) in methanol (50.0 mL) was refluxed for 2 h, and then the reaction mixture was concentrated. The residue was taken up between ethyl acetate and saturated aqueous sodium chloride. The separated organic layer was washed with water and brine, dried over sodium sulfate and filtered. The filtrate was treated by flash column chromatography on silica gel with *n*-hexane as eluent to give 5-(4-bromophenyl)oxazole (1.63 g, 73%) as a brown solid.

To a reaction tube with a magnetic stir bar, $\text{Pd}(\text{PPh}_3)_4$ (5 mol%, 57.8 mg, 50 μmol), 5-(4-bromophenyl)oxazole (224 mg, 1.0 mmol) and 4-(diphenylamino)phenylboronic acid (346.8 mg, 1.2 mmol), K_2CO_3 (276 mg, 2.0 mmol), toluene (3.0 mL), EtOH (1.0

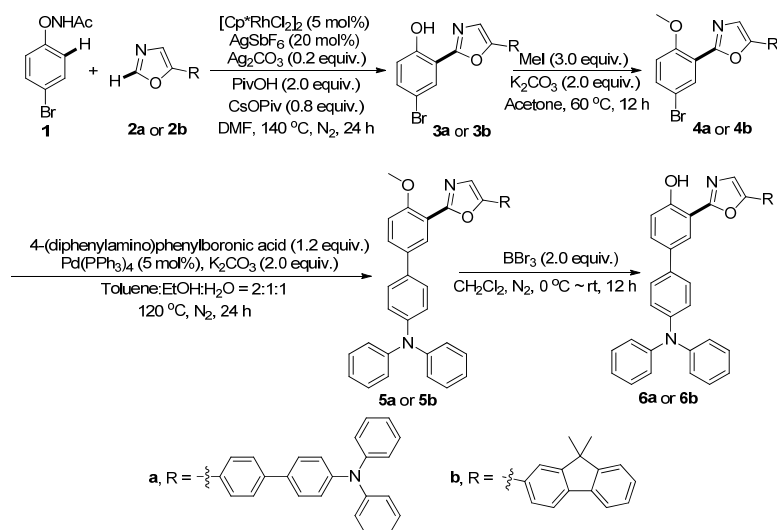
mL) and H₂O (1.0 mL) were added under an N₂ atmosphere. The reaction mixture was stirred at 120 °C for 24 h. The reaction mixture was then cooled to ambient temperature, filtered through a celite pad, and washed with 20 mL of dichloromethane. Organic solvent was removed under reduced pressure. The residue was purified by flash column chromatography (petroleum ether/ethyl acetate = 4/1, v/v) to afford the desired product as a pale yellow solid (353.4 mg, 91%).

2.3 Synthesis of 5-(9,9-dimethyl-9H-fluoren-2-yl)oxazole (2b)²



Scheme S3. Synthetic route to compound **2b**. [P]: butyldi-1-adamantylphosphine.

5-(9,9-Dimethyl-9H-fluoren-2-yl)oxazole was synthesized according to literature reports.^[2] In a 10 mL flame-dried Schlenk tube with a magnetic stir bar was charged with 2-bromo-9,9-dimethyl-9H-fluorene (546 mg, 2.0 mmol, 1.0 equiv.), Pd(OAc)₂ (22 mg, 0.1 mmol), K₂CO₃ (828 mg, 6.0 mmol, 3.0 equiv.), butyldi-1-adamantylphosphine (71.6 mg, 0.2 mmol), pivalic acid (PivOH, 82 mg, 0.8 mmol), oxazole (263 μL, 4.0 mmol, 1.5 equiv.) and DMAc (9.0 mL). The test tube was submerged in an oil bath and was stirred at 110 °C for 16 h. After cooling to room temperature, DMAc was removed by decompression, and reaction mixtures were purified by column chromatography on silica gel with petroleum ether/EtOAc = 5:1 (v/v) as eluent to get the target product (267 mg, 51%).



Scheme S4. Synthetic route of 2-(2'-hydroxyphenyl)oxazoles **6a** and **6b**.

2.4 Synthesis of **3a** and **3b**¹

N-(4-Bromophenoxy)acetamide(**1**) (57 mg, 0.25 mmol), [Cp*RhCl₂]₂ (8 mg, 5 mol%), 5-aryloxazole (**2a**: 116 mg; **2b**: 78 mg, 0.3 mmol), AgSbF₆ (17 mg, 20 mol%), Ag₂CO₃ (14 mg, 0.2 equiv.), PivOH (51 mg, 2.0 equiv.) and CsOPiv (47 mg, 0.8 equiv.) were added into a 25 mL flame-dried Schlenk tube with a magnetic stir bar, to which was added DMF (1.0 mL). The reaction vessel was stirred at 140 °C for 24 h. Then the mixture was filtered off and washed with dichloromethane. The solvent was then washed three times with saturated salt water. The organic phase was dried with Na₂SO₄ and removed under reduce pressure. The residue was purified by column chromatography on silica gel to afford the corresponding product (**3a**: 80 mg, 57%; **3b**: 77 mg, 71%).

2.5 Synthesis of **4a** and **4b**

2-(2'-Hydroxyphenyl)oxazole derivatives (**3a** or **3b**) (**3a**: 449 mg; **3b**: 431 mg, 1.0 mmol) dissolved in acetone (0.1 M), K₂CO₃ (2.0 equiv.) and MeI (3.0 equiv.) was added, respectively. The mixture was stirred at 60 °C for 12 h. After cooling to room temperature, the mixture was filtered off and washed with dichloromethane. The solvent was then removed under reduced pressure. The residue was used in next step after recrystallization with ethanol (**4a**: 440 mg, 95%; **4b**: 409 mg, 92%).

2.6 Synthesis of **5a** and **5b**

To a reaction tube with a magnetic stir bar, Pd(PPh₃)₄ (57.8 mg, 5 mol%), **4a** or **4b** (**4a**: 463 mg; **4b**: 445 mg, 1.0 mmol) and 4-(diphenylamino)phenylboronic acid (346.8 mg, 1.2 mmol), K₂CO₃ (276.0 mg, 2.0 equiv.), toluene (5.0 mL), EtOH (1.0 mL) and H₂O (1.0 mL) were added under an N₂ atmosphere. The reaction mixture was stirred at 120 °C for 24 h. The reaction mixture was then cooled to ambient temperature, filtered through a celite pad, and washed with 20 mL of dichloromethane. Organic solvent was removed under reduced pressure. The residue was purified by flash column chromatography with petroleum ether/dichloromethane/EtOAc = 5:1:1 (v/v/v) to afford the desired product (**5a**: 620 mg, 84%; **5b**: 532 mg, 87%).

2.7 Synthesis of **6a** and **6b**³

To a reaction tube with a magnetic stir bar, **5a** or **5b** (**5a**: 74 mg; **5b**: 61 mg, 0.1 mmol) was dissolved in super dry dichloromethane (20.0 mL) under an N₂ atmosphere in an ice bath, BBr₃ (19 μL, 2.0 equiv.) was diluted with super dry dichloromethane (5.0 mL) and slowly added to the reaction tube. The reaction was slowly warmed to room temperature and stirred for 12 h. The reaction was quenched with MeOH, filtered through a celite pad, and washed with 20 mL dichloromethane. Organic solvent was removed under reduced pressure. The residue was purified by flash column chromatography with petroleum ether/dichloromethane/EtOAc = 10:1:1 (v/v/v) to afford the desired product (**6a**: 66 mg, 91%; **6b**: 49 mg, 82%).

III. Steady-state and time-resolved photophysical properties of **6a** and **6b**

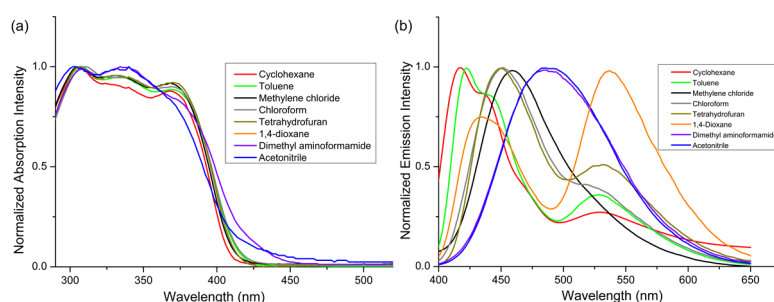


Figure S1. Normalized UV-Vis absorption spectra (1.0 × 10⁻⁶ M) and fluorescence emission spectra (5.0 × 10⁻⁵ M) of **6a** in different solvents.

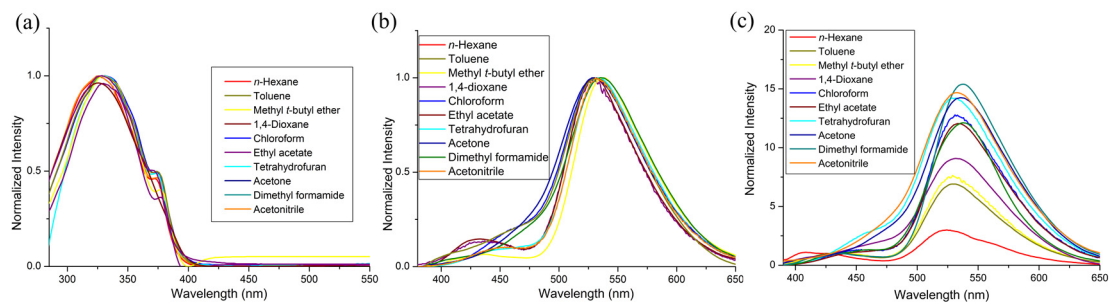


Figure S2. (a) Normalized UV-Vis absorption spectra (1.0×10^{-6} M) of **6b** in different solvents; (b) Fluorescence emission spectra normalized with keto-form emission peaks (5.0×10^{-5} M) of **6b** in different solvents; (c) Fluorescence emission spectra normalized with enol-form emission peaks (5.0×10^{-5} M) of **6b** in different solvents.

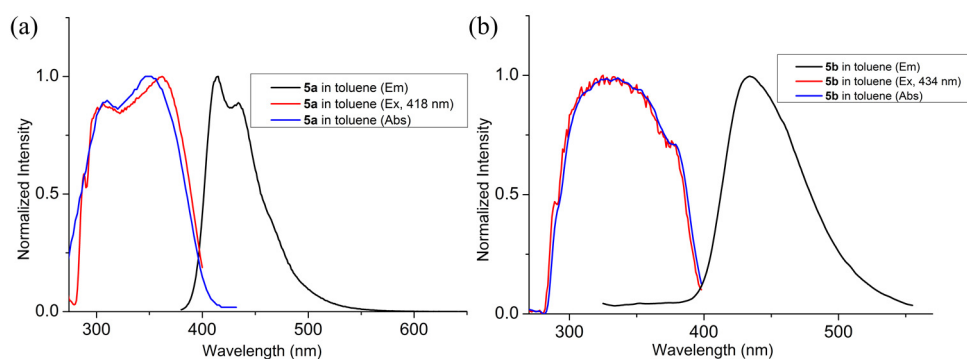


Figure S3. Normalized fluorescence emission spectra (black line, 5×10^{-5} M), absorption spectra (blue line, 1×10^{-6} M) and excitation spectra (red line, 5×10^{-5} M) of **5a** and **5b** in toluene at room temperature with monitored emission wavelength as depicted.

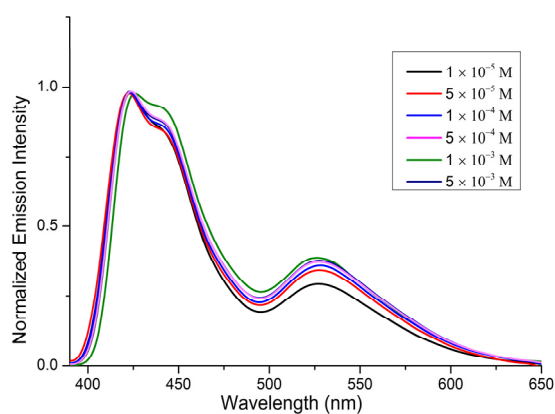


Figure S4. Normalized fluorescence emission spectra of **6a** in toluene with different concentrations.

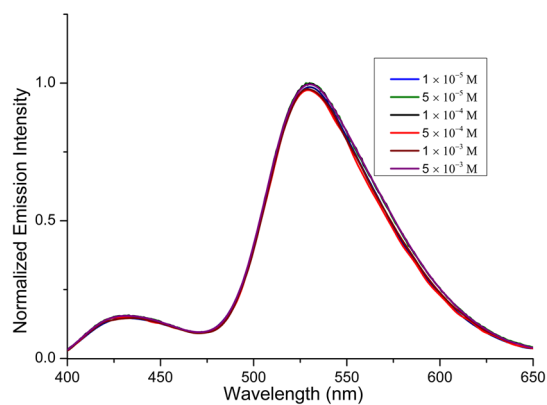


Figure S5. Normalized fluorescence emission spectra of **6b** in toluene with different concentrations.

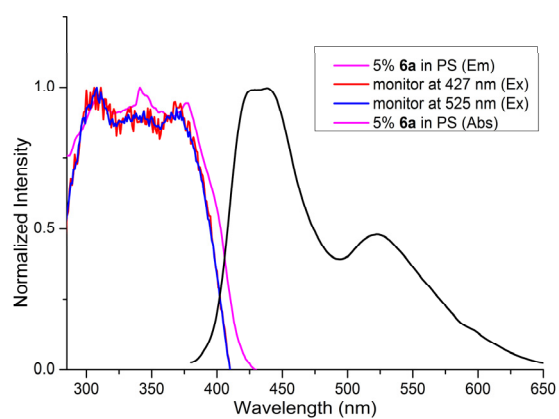


Figure S6. Normalized fluorescence emission spectra (back line), absorption spectra (pink line) and excitation spectra (red line and blue line) of **6a** in PS film (5% wt) at room temperature with monitored emission wavelength as depicted.

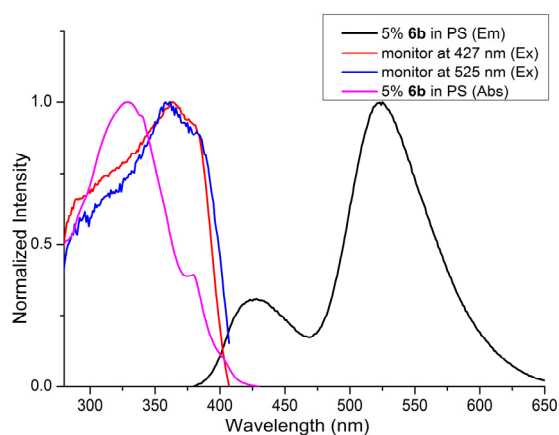


Figure S7. Normalized fluorescence emission spectra (back line), absorption spectra (pink line) and excitation spectra (red line and blue line) of **6b** in PS film (5% wt) at room temperature with monitored emission wavelength as depicted.

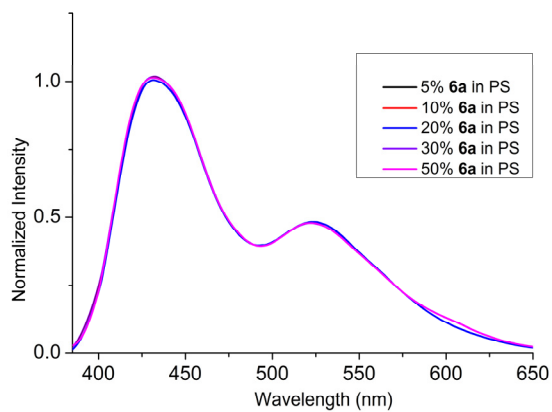


Figure S8. Normalized fluorescence emission spectra of **6a** in PS film with different concentration.

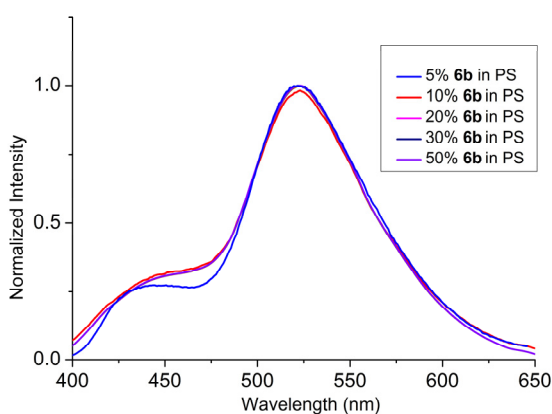


Figure S9. Normalized fluorescence emission spectra of **6b** in PS film with different concentration.

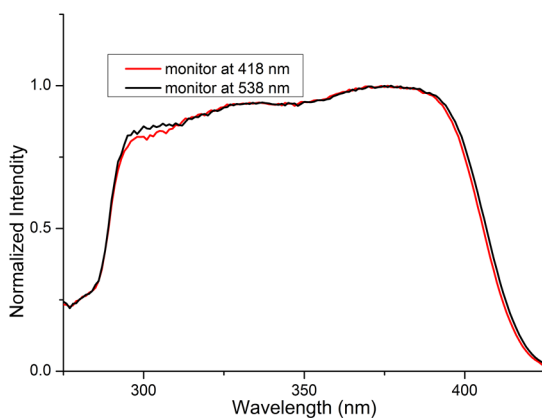


Figure S10. Normalized excitation spectra of **6a** in toluene (5×10^{-5} M) at room temperature with monitored emission wavelength as depicted.

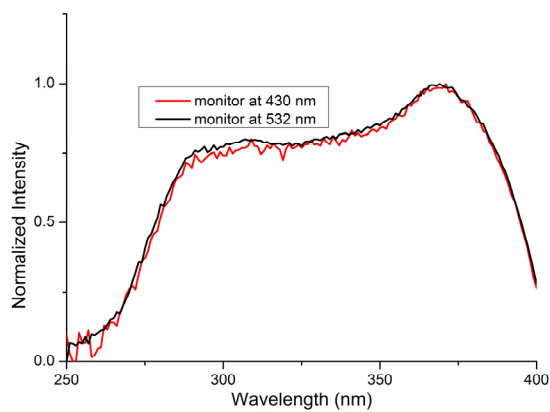


Figure S11. Normalized excitation spectra of **6a** in tetrahydrofuran (5×10^{-5} M) at room temperature with monitored emission wavelength as depicted.

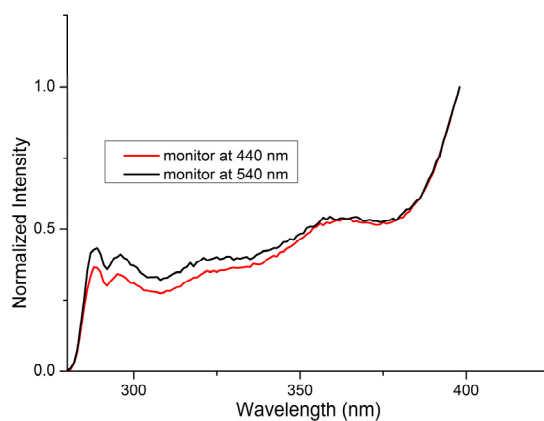


Figure S12. Normalized excitation spectra of **6a** in 1,4-dioxane (5×10^{-5} M) at room temperature with monitored emission wavelength as depicted.

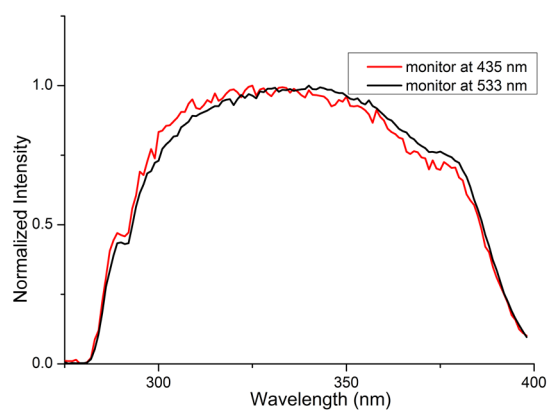


Figure S13. Normalized excitation spectra of **6b** in toluene (5×10^{-5} M) at room temperature with monitored emission wavelength as depicted.

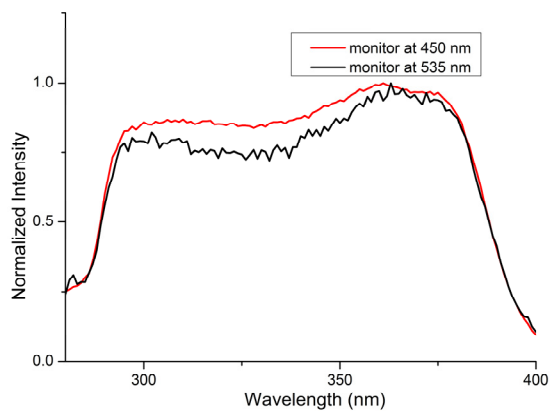


Figure S14. Normalized excitation spectra of **6b** in tetrahydrofuran (5×10^{-5} M) at room temperature with monitored emission wavelength as depicted.

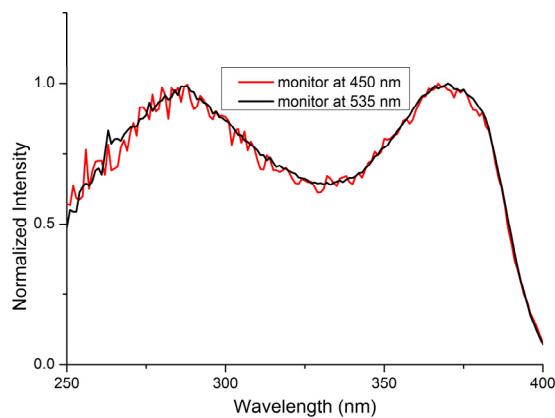


Figure S15. Normalized excitation spectra of **6b** in 1,4-dioxane (5×10^{-5} M) at room temperature with monitored emission wavelength as depicted.

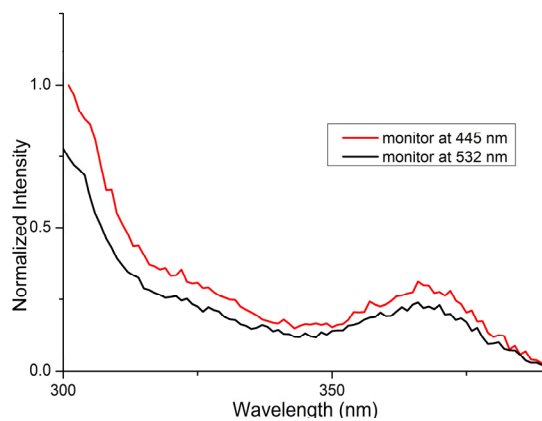


Figure S16. Normalized excitation spectra of pristine **6a** at room temperature with monitored emission wavelength as depicted.

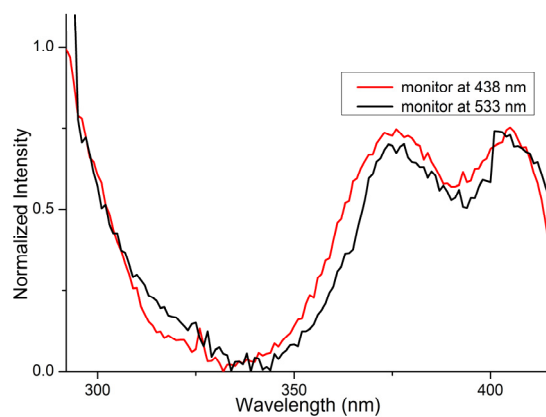


Figure S17. Normalized excitation spectra of pristine **6b** at room temperature with monitored emission wavelength as depicted.

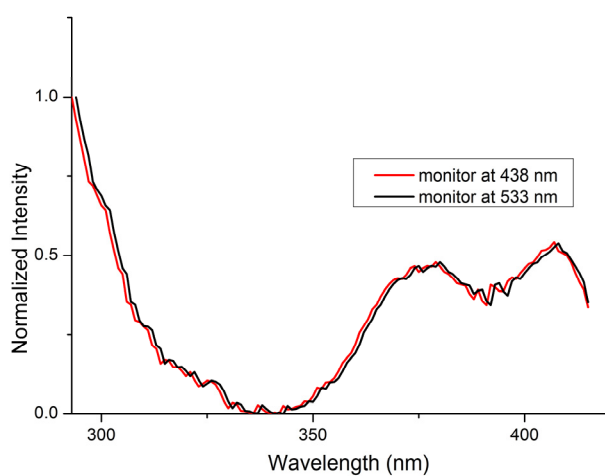


Figure S18. Normalized excitation spectra of ground **6b** at room temperature with monitored emission wavelength as depicted.

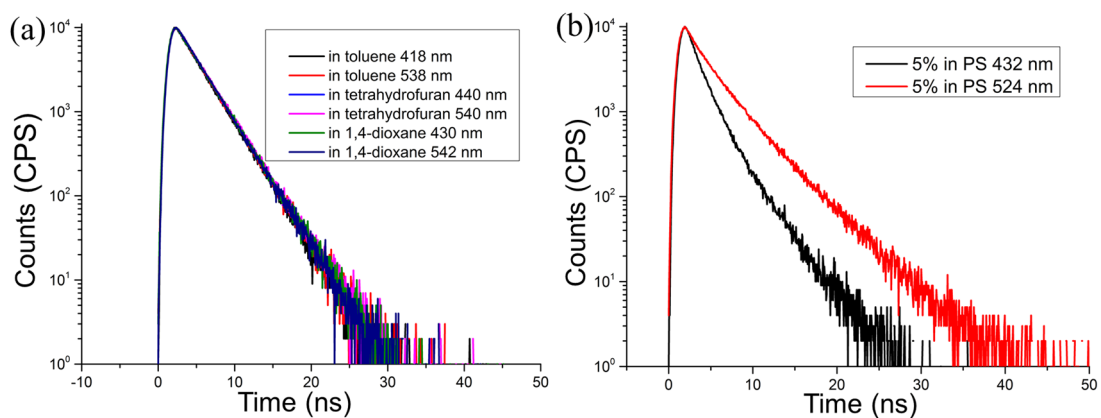


Figure S19. Time-correlated single photon counting measurement of **6a** in different solvents (5×10^{-5} M) (a) and in PS film (5% wt) (b) at room temperature. The data were acquired at $\lambda_{\text{ex}} = 370$ nm.

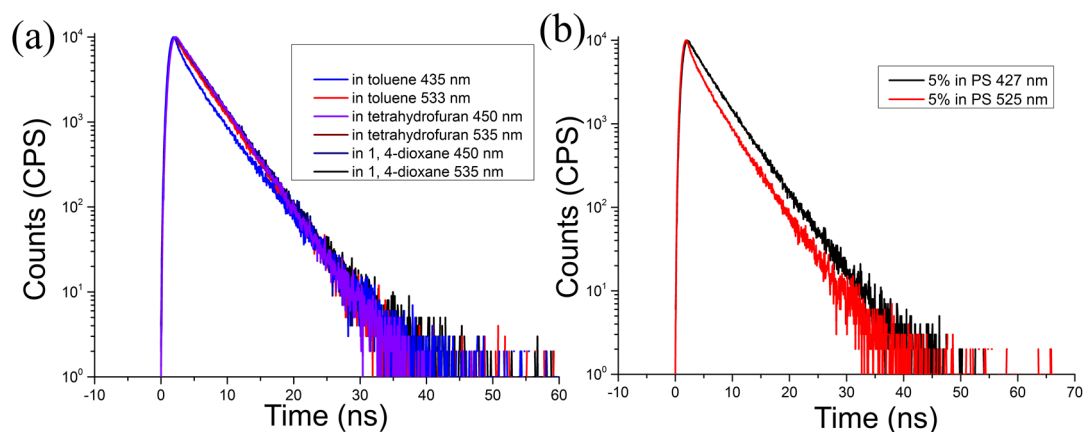


Figure S20. Time-correlated single photon counting measurement of **6b** in different solvents (5×10^{-5} M) (a) and in PS film (5% wt) (b) at room temperature. The data were acquired at $\lambda_{\text{ex}} = 370$ nm.

Table S1. Time-resolved photophysical (TCSPC) properties of **6a** and **6b**

TCSPC measurement			TCSPC measurement				
state	λ_{em}	τ	state	λ_{em}	τ		
6a	in toluene	418 nm	2.9 ± 0.1 ns	6b	in toluene	435 nm	3.7 ± 0.1 ns
		538 nm	3.0 ± 0.1 ns		in toluene	533 nm	3.8 ± 0.2 ns
	in THF	440 nm	2.9 ± 0.1 ns		in THF	450 nm	3.8 ± 0.2 ns
		540 nm	2.9 ± 0.1 ns		in THF	535 nm	3.8 ± 0.1 ns
	in 1,4-dioxane	430 nm	2.9 ± 0.1 ns		in 1,4-dioxane	450 nm	3.8 ± 0.2 ns
		542 nm	3.0 ± 0.1 ns		in 1,4-dioxane	535 nm	3.9 ± 0.2 ns
in PS	432 nm	2.1 ± 0.2 ns	in PS	427 nm	3.9 ± 0.3 ns		
	534 nm	3.6 ± 0.2 ns	in PS	525 nm	4.4 ± 0.3 ns		

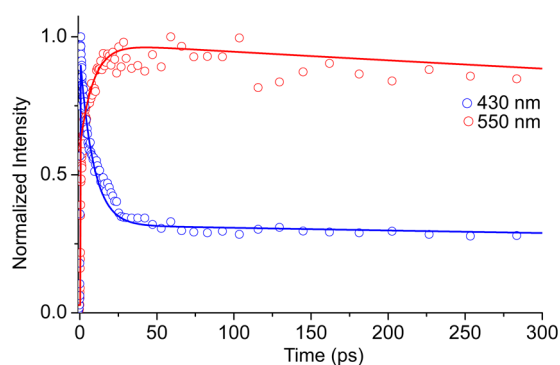


Figure S21. Fluorescence up-conversion decay curves of **6a** in toluene (5×10^{-5} M) at room temperature. The data were acquired at $\lambda_{\text{ex}} = 350$ nm and the data points are shown with monitored emission wavelength as depicted. Solid lines depict the best biexponential fits.

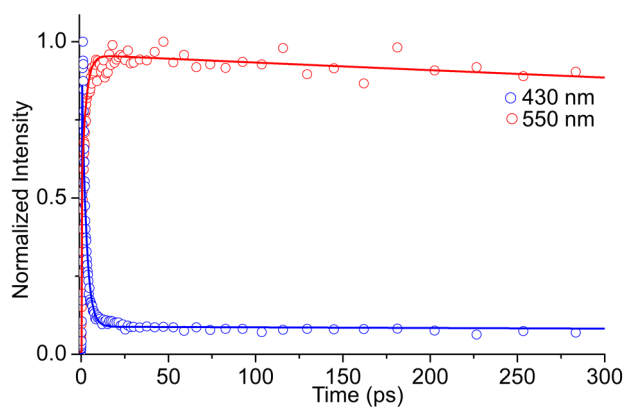
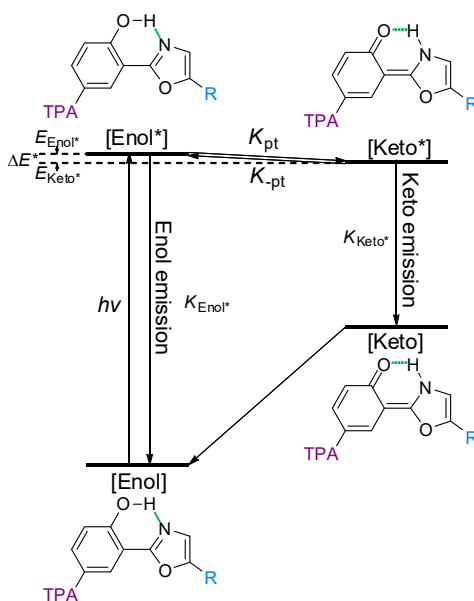


Figure S22. Fluorescence up-conversion decay curves of **6b** in toluene (5×10^{-5} M) at room temperature. The data were acquired at $\lambda_{\text{ex}} = 350$ nm and the data points are shown with monitored emission wavelength as depicted. Solid lines depict the best biexponential fits.

IV. Kinetic derivation and calculation of reversible ESIPT reaction



Scheme S5. Reversible ESIPT reaction model for **6a** and **6b**. [Enol*]: concentration of excited-state enol-form species; [Keto*]: concentration of excited-state keto-form species; K_{pt} : proton transfer rate constant; $K_{-\text{pt}}$: reverse proton-transfer rate constant; K_{Enol^*} : decay rate constant of excited-state enol-form species for all decay channel except K_{pt} ; K_{Keto^*} : decay rate constant of excited-state keto-form species for all decay channel except $K_{-\text{pt}}$; E_{Enol^*} : the free energy of enol-form excited state; E_{Keto^*} : the free energy of keto-form excited state; $\Delta E^* = E_{\text{Keto}^*} - E_{\text{Enol}^*}$.

According to the reaction model, the differential rate equations for change of concentrations of enol-form and keto-form species can be expressed as follows:

$$\frac{d[\text{Enol}^*]}{dt} = -(K_{\text{Enol}^*} + K_{\text{pt}})[\text{Enol}^*] + K_{\text{-pt}}[\text{Keto}^*] \quad (1)$$

$$\frac{d[\text{Keto}^*]}{dt} = -(K_{\text{Keto}^*} + K_{\text{-pt}})[\text{Keto}^*] + K_{\text{pt}}[\text{Enol}^*] \quad (2)$$

The coupling equations (1) and (2) can be solved with given initial conditions,

$$[\text{Enol}^*]_{(t)} = [\text{Enol}^*]_0 \text{ and } [\text{Keto}^*]_{(t)} = [\text{Keto}^*]_0 = 0 \text{ at } t = 0$$

$$[\text{Enol}^*]_{(t)} = \frac{e^{1/2(a-A+d)t}[d-de^{At}+a(-1+e^{At})+A(1+e^{At})][\text{Enol}^*]_0}{2A} \quad (3)$$

$$[\text{Keto}^*]_{(t)} = \frac{ce^{1/2(a-A+d)t}(-1+e^{At})[\text{Enol}^*]_0}{A} \quad (4)$$

$$\text{with } a = -K_{\text{pt}} - K_{\text{Enol}^*}$$

$$b = K_{\text{-pt}}$$

$$c = K_{\text{pt}}$$

$$d = -K_{\text{-pt}} - K_{\text{Keto}^*}$$

$$A = \sqrt{a^2 + 4bc - 2ad + d^2}$$

Equations (3) and (4) can be rewritten as follows:

$$[\text{Enol}^*]_{(t)} = \frac{[\text{Enol}^*]_0}{2A} \left[(d - a + A)e^{\frac{(a-A+d)t}{2}} + (a + A - d)e^{\frac{(a+A+d)t}{2}} \right] \quad (5)$$

$$[\text{Keto}^*]_{(t)} = \frac{c[\text{Enol}^*]_0}{A} \left[e^{\frac{(a+A+d)t}{2}} - e^{\frac{(a-A+d)t}{2}} \right] \quad (6)$$

Equations (5) and (6) can be transformed with $\lambda_1 = \frac{-(a+A+d)}{2}$, $\lambda_2 = \frac{-(a-A+d)}{2}$

$$[\text{Enol}^*]_{(t)} = \frac{[\text{Enol}^*]_0}{\lambda_2 - \lambda_1} \left[(\lambda_2 + a)e^{-\lambda_1 t} + (-\lambda_1 - a)e^{-\lambda_2 t} \right] \quad (7)$$

$$[\text{Keto}^*]_{(t)} = \frac{K_{\text{pt}}[\text{Enol}^*]_0}{\lambda_2 - \lambda_1} \left[e^{-\lambda_1 t} - e^{-\lambda_2 t} \right] \quad (8)$$

Under the assumption that there exists a fast, excited-state equilibrium between the enol-form and keto-form species (i.e. K_{pt} and $K_{\text{-pt}} \gg K_{\text{Enol}^*}$ and K_{Keto^*}),

So

$$\lambda_1 = \frac{K_{\text{Enol}^*} + K_{\text{eq}}K_{\text{Keto}^*}}{1 + K_{\text{eq}}} \quad (9)$$

$$\lambda_2 = K_{\text{pt}} + K_{\text{-pt}} \quad (10)$$

$$\text{with } K_{\text{eq}} = \frac{K_{\text{pt}}}{K_{\text{-pt}}}$$

For the time-resolved enol-form emission ($[\text{Enol}^*]_{(t)}$), λ_1 and λ_2 represent slow

population decay rate constants and the sum of reversible proton transfer rate ($K_{pt} + K_{-pt}$), respectively. The pre-exponential factors contributed to fast and slow decay components of $[\text{Enol}^*]_{(t)}$, denoted as $[\text{Enol}^*]_{\text{fast}}$ and $[\text{Enol}^*]_{\text{slow}}$, respectively. Therefore, the time-resolved $[\text{Enol}^*]_{(t)}$ and $[\text{Keto}^*]_{(t)}$ can be expressed as shown

$$[\text{Enol}^*]_{(t)} = [\text{Enol}^*]_0 [A_1 e^{-t/\tau_1} + A_2 e^{-t/\tau_2}] \quad (11)$$

$$[\text{Keto}^*]_{(t)} = \frac{K_{pt}[\text{Enol}^*]_0}{\frac{1}{\tau_2} - \frac{1}{\tau_1}} [e^{-t/\tau_1} - e^{-t/\tau_2}] \quad (12)$$

with

$$A_1 = \frac{K_{-pt}}{K_{pt} + K_{-pt}}$$

$$A_2 = \frac{K_{pt}}{K_{pt} + K_{-pt}}$$

hence

$$K_{\text{eq}} = \frac{K_{pt}}{K_{-pt}} = \frac{A_2}{A_1} \quad (13)$$

$$\frac{1}{\tau_1} = \frac{K_{\text{Enol}^*} + K_{\text{eq}}K_{\text{Keto}^*}}{1 + K_{\text{eq}}} \quad (14)$$

$$\frac{1}{\tau_2} = K_{pt} + K_{-pt} \quad (15)$$

Calculation for **6a**:

$$K_{\text{eq}} = \frac{K_{pt}}{K_{-pt}} = \frac{A_2}{A_1} = \frac{0.67}{0.33} = 2.0$$

$$\frac{1}{\tau_2} = K_{pt} + K_{-pt} = \frac{1}{8.7} = 0.115$$

hence

$$K_{pt} = 0.076, \quad \tau_{pt} = \frac{1}{K_{pt}} = 13.2, \quad K_{-pt} = 0.038, \quad \tau_{-pt} = \frac{1}{K_{-pt}} = 26.3$$

$$\Delta E^* = E_{\text{keto}^*} - E_{\text{Enol}^*} = -RT \ln K_{\text{eq}} = -0.41 \text{ kcal/mol}$$

Calculation for **6b**:

$$K_{\text{eq}} = \frac{K_{pt}}{K_{-pt}} = \frac{A_2}{A_1} = \frac{0.94}{0.06} = 15.6$$

$$\frac{1}{\tau_2} = K_{pt} + K_{-pt} = \frac{1}{2.5} = 0.4$$

hence

$$K_{\text{pt}} = 0.374, \quad \tau_{\text{pt}} = \frac{1}{K_{\text{pt}}} = 2.7, \quad K_{-\text{pt}} = 0.024, \quad \tau_{-\text{pt}} = \frac{1}{K_{-\text{pt}}} = 41.7$$

$$\Delta E^* = E_{\text{keto}^*} - E_{\text{Enol}^*} = -RT \ln K_{\text{eq}} = -1.64 \text{ kcal/mol}$$

Calculation for pristine **6b**:

$$K_{\text{eq}} = \frac{K_{\text{pt}}}{K_{-\text{pt}}} = \frac{A_2}{A_1} = \frac{0.79}{0.20} = 4.0$$

$$\frac{1}{\tau_2} = K_{\text{pt}} + K_{-\text{pt}} = \frac{1}{4.5} = 0.222$$

hence

$$K_{\text{pt}} = 0.179, \quad \tau_{\text{pt}} = \frac{1}{K_{\text{pt}}} = 5.6, \quad K_{-\text{pt}} = 0.044, \quad \tau_{-\text{pt}} = \frac{1}{K_{-\text{pt}}} = 22.5$$

$$\Delta E^* = E_{\text{keto}^*} - E_{\text{Enol}^*} = -RT \ln K_{\text{eq}} = -0.83 \text{ kcal/mol}$$

Calculation for ground powder of white-emitting crystal of **6b**:

$$K_{\text{eq}} = \frac{K_{\text{pt}}}{K_{-\text{pt}}} = \frac{A_2}{A_1} = \frac{0.76}{0.23} = 3.3$$

$$\frac{1}{\tau_2} = K_{\text{pt}} + K_{-\text{pt}} = \frac{1}{4.1} = 0.244$$

hence

$$K_{\text{pt}} = 0.189, \quad \tau_{\text{pt}} = \frac{1}{K_{\text{pt}}} = 5.3, \quad K_{-\text{pt}} = 0.057, \quad \tau_{-\text{pt}} = \frac{1}{K_{-\text{pt}}} = 17.6$$

$$\Delta E^* = E_{\text{keto}^*} - E_{\text{Enol}^*} = -RT \ln K_{\text{eq}} = -0.71 \text{ kcal/mol}$$

Table S2. Photophysical properties of **6a** and **6b** in toluene at room temperature

	steady-state measurement			femtosecond fluorescence up-conversion measurement ^[a]					
	λ_{abs} (nm)	λ_{em} (nm)	Φ_f	λ_{monitor}	τ_{obs} (pre-exp. factor) ^[b]	$\tau_{\text{pt}}^{\text{pt}}$ (k_{pt}^{-1})	$\tau_{-\text{pt}}^{\text{pt}}$ ($k_{-\text{pt}}^{-1}$)	K_{eq}	ΔE^* ^[c]
6a	300, 336, 368	Enol: 418, 433	0.63	430 nm	8.7 ps (0.67), 2.9 ns (0.33) ^[d]	13.2 ps	26.3 ps	2.0	-0.41 kcal/mol
		Keto: 538		550 nm	8.7 ps (-0.38), 2.9 ns (0.95) ^[d]				
6b	330, 372	Enol: 435	0.52	430 nm	2.5 ps (0.94), 3.8 ns (0.06) ^[d]	2.7 ps	41.7 ps	15.6	-1.64 kcal/mol
		Keto: 533		550 nm	2.5 ps (-0.55), 3.8 ns (0.93) ^[d]				

[a] k_{pt} : proton transfer rate constant; $k_{-\text{pt}}$: reverse proton-transfer rate constant; $K_{\text{eq}} = k_{\text{pt}}/k_{-\text{pt}}$, equilibrium constant. [b] Observed emission lifetimes (τ_{obs}) by femtosecond fluorescence up-conversion. [c] $\Delta E^* = E_{\text{keto}^*} - E_{\text{Enol}^*}$; E_{Enol^*} : free energy of enol-form excited state; E_{keto^*} : free energy of keto-form excited state. [d] Population decay time constant was applied for the fitting by nanosecond time-correlated single-photon counting technique.

V. Characterization of mechanochromism

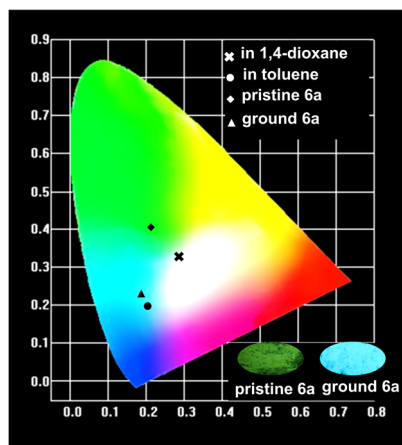


Figure S23. Emission color coordinates of **6a** in the CIE 1931 chromaticity diagram: in 1,4-dioxane (0.29, 0.35); in toluene (0.20, 0.20); pristine **6a** (0.20, 0.40) and ground **6a** (0.19, 0.23).

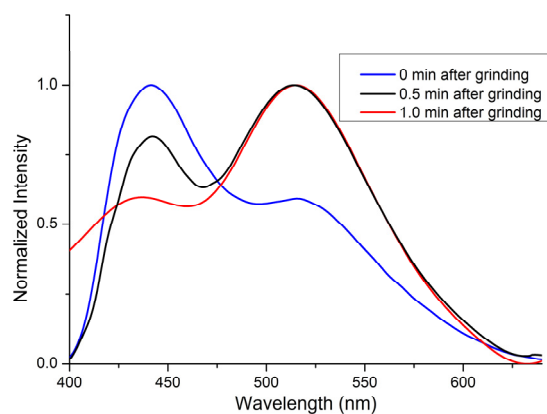


Figure S24. Normalized fluorescence emission spectra of **6a** with different time after grinding.

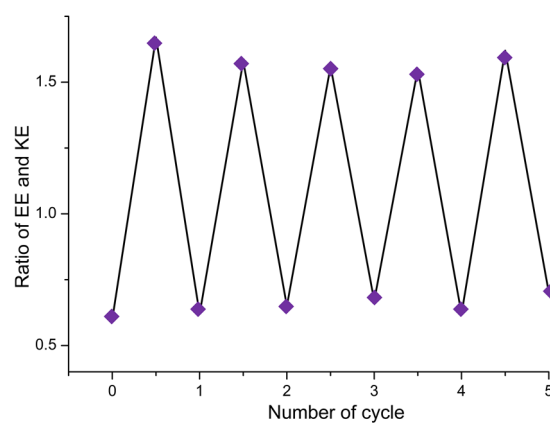


Figure S25. Reversible switching of emission of **6a** (EE: enol-form emission; KE: keto-form emission).

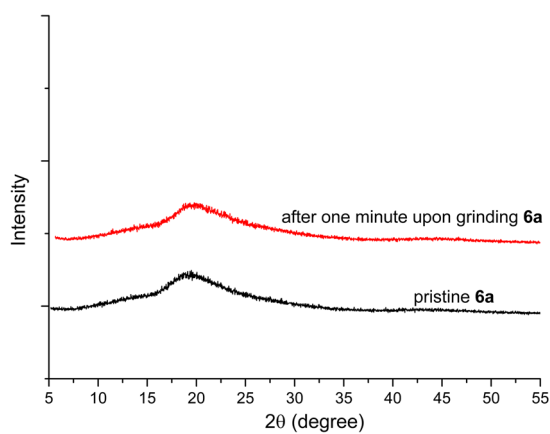


Figure S26. PXRD patterns of **6a**.

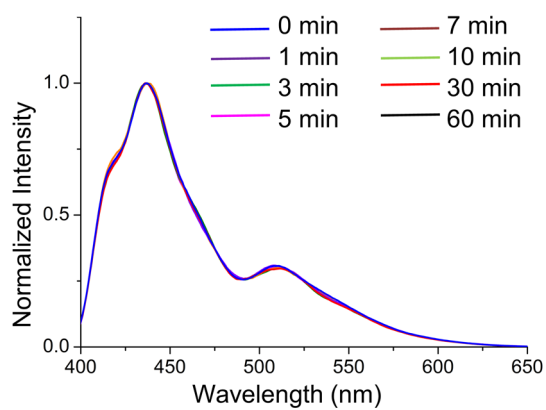


Figure S27. Normalized fluorescence emission spectra of ground **6a** in liquid nitrogen with different time.

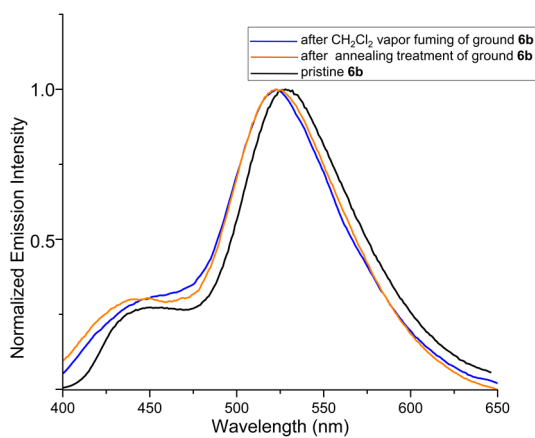


Figure S28. Normalized fluorescence emission spectra of pristine **6b**, after CH_2Cl_2 vapor fuming and annealing treatment of ground **6b**.

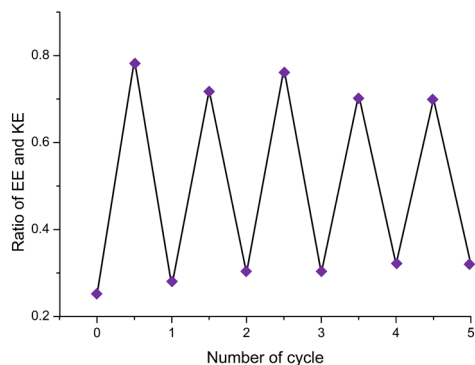


Figure S29. Reversible switching of emission of **6b** by repeated grinding-CH₂Cl₂ vapor fuming cycles (EE: enol-form emission; KE: keto-form emission).

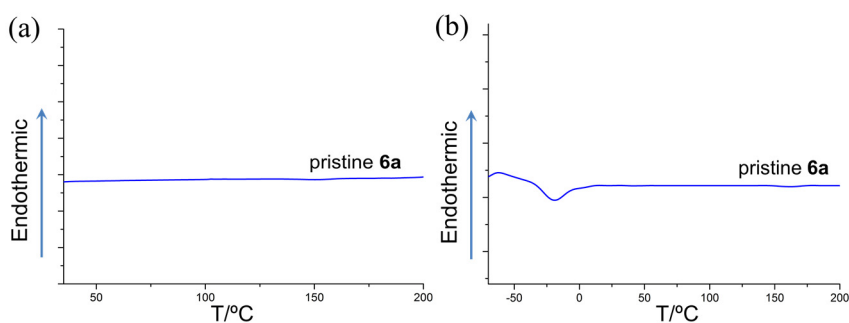


Figure S30. DSC curves of pristine **6a** from room temperature to 200 °C (a) and from -75 °C to 200 °C (b) at a heating rate of 5 °C/min.

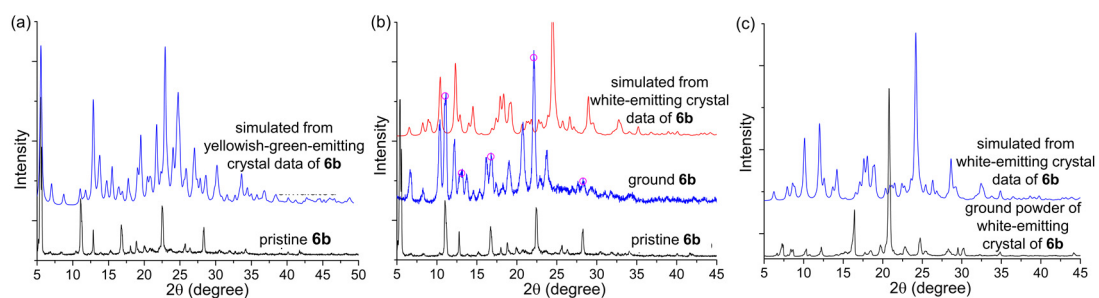


Figure S31. a) PXRD pattern obtained from the yellowish-green-emitting single-crystal data of **6b** and pristine **6b**; b) PXRD patterns obtained from the white-emitting single-crystal data of **6b**, ground **6b** and pristine **6b**; c) PXRD patterns obtained from the white-emitting single-crystal data of **6b** and ground powder of white-emitting crystal of **6b**.

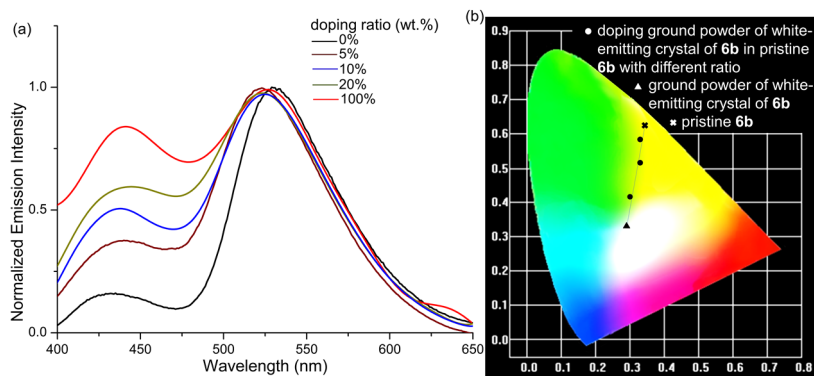


Figure S32. a) Normalized fluorescence emission spectra of mixed simples (Doping ground powder of white-emitting crystal of **6b** in pristine **6b** with the ratio of 0, 5, 10, 20, 100%, respectively). b) Emission color coordinates in CIE 1931 chromaticity diagram of mixed simples (Doping ground powder of white-emitting crystal of **6b** in pristine **6b** with the ratio of 0, 5, 10, 20, 100%, respectively). Pristine **6b** (0.32, 0.62). Doping ratios: 5% (0.31, 0.57), 10% (0.31, 0.53), and 20% (0.30, 0.43). Ground powder of white-emitting crystal of **6b** (0.28, 0.34).

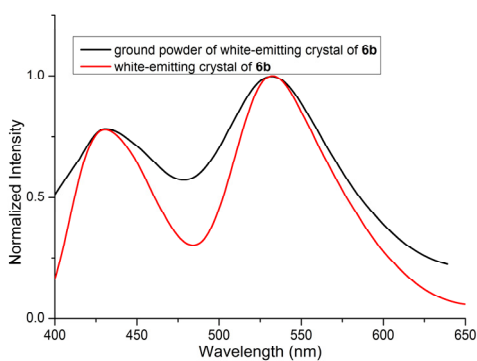


Figure S33. Normalized fluorescence emission spectra of white-emitting crystal of **6b** and ground powder of white-emitting crystal of **6b**.

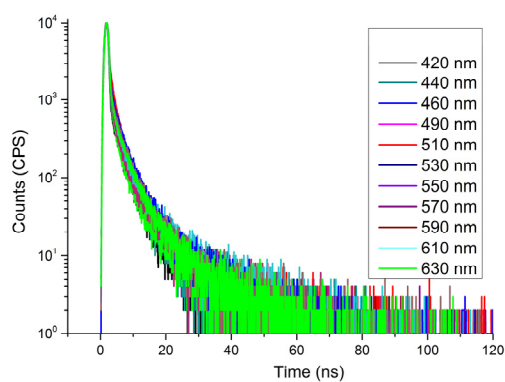


Figure S34. Time-correlated single photon counting measurement of yellowish-green-emitting crystal of **6b** at room temperature. The data were acquired at $\lambda_{ex}= 370$ nm.

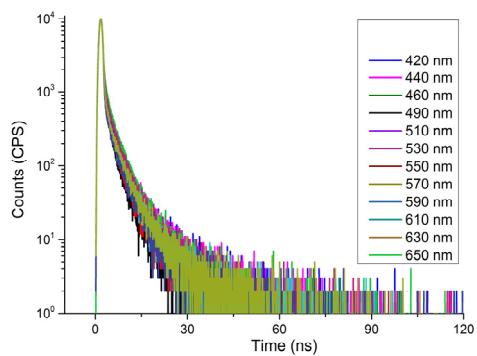


Figure S35. Time-correlated single photon counting measurement of white-emitting crystal of **6b** at room temperature. The data were acquired at $\lambda_{\text{ex}}=370$ nm.

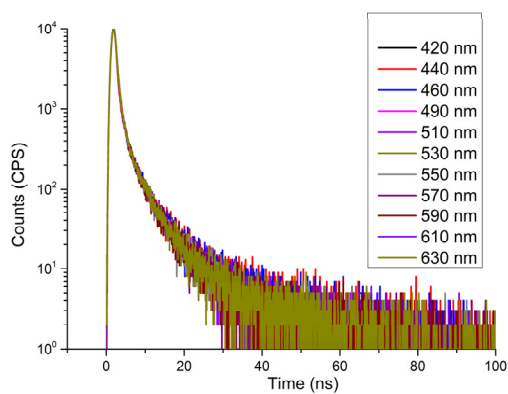


Figure S36. Time-correlated single photon counting measurement of pristine **6b** at room temperature. The data were acquired at $\lambda_{\text{ex}}=370$ nm.

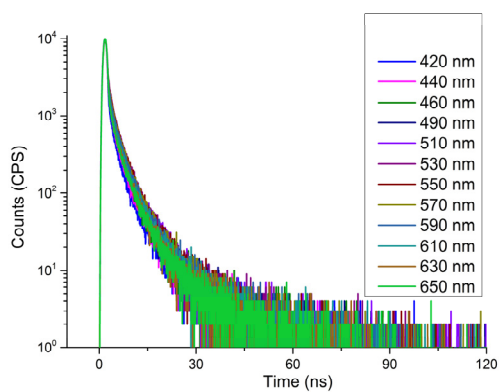


Figure S37. Time-correlated single photon counting measurement of ground **6b** at room temperature. The data were acquired at $\lambda_{\text{ex}}=370$ nm.

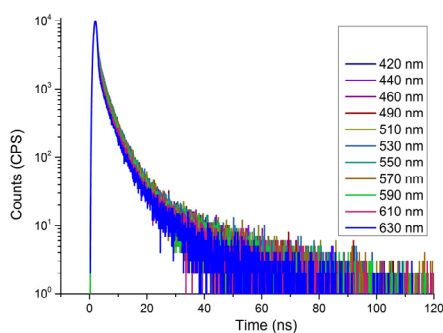


Figure S38. Time-correlated single photon counting measurement of ground powder of white-emitting crystals of **6b** at room temperature. The data were acquired at $\lambda_{\text{ex}}=370$ nm.

Table S3. Time-resolved photophysical properties of **6b** in different state

time-correlated single photon counting measurement			
state	λ_{monitor}	τ_1	τ_2
Yellowish-green-emitting crystal of 6b	440 nm	0.3 ± 0.03 ns (0.98)	3.5 ± 0.1 ns (0.02)
	530 nm	0.3 ± 0.03 ns (0.98)	3.5 ± 0.1 ns (0.02)
Pristine 6b	440 nm	0.3 ± 0.04 ns (0.97)	3.6 ± 0.1 ns (0.03)
	530 nm	0.3 ± 0.03 ns (0.97)	3.6 ± 0.1 ns (0.03)
Ground 6b	440 nm	0.3 ± 0.05 ns (0.93)	3.6 ± 0.1 ns (0.07)
	530 nm	0.3 ± 0.03 ns (0.93)	3.6 ± 0.1 ns (0.07)
White-emitting crystal of 6b	440 nm	0.3 ± 0.04 ns (0.99)	3.5 ± 0.1 ns (0.01)
	530nm	0.3 ± 0.02 ns (0.99)	3.5 ± 0.1 ns (0.01)
Ground powder of white-emitting crystal of 6b	440 nm	0.3 ± 0.06 ns (0.92)	3.6 ± 0.1 ns (0.08)
	530 nm	0.3 ± 0.04 ns (0.92)	3.7 ± 0.1 ns (0.08)

VI. TGA curves of 6a and 6b

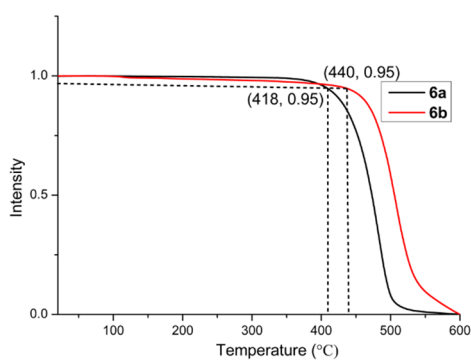


Figure S39. TGA curves of **6a** and **6b** recorded at a heating rate of 10 °C/min under an N_2 atmosphere.

VII. Crystal data

The yellowish-green-emitting single crystals of **6b** were acquired by slow solvent evaporation of **6b** in the mixed solvent of CH₂Cl₂ and CH₃CN in room temperature. The white-emitting single crystals of **6b** were acquired by temperature gradient vacuum sublimation using vacuum purification device (ZTS-100-I) at 300 °C.

Table S4. Crystal Data for the yellowish-green-emitting single crystal of **6b**.

Identification code	yjs-hq-6b
Empirical formula	C ₄₃ H ₃₄ Cl ₂ N ₂ O ₂
Formula weight	681.62
Temperature/K	294.1(3)
Crystal system	monoclinic
Space group	P2 ₁ /c
a/Å	8.09943(19)
b/Å	31.2756(9)
c/Å	13.9351(5)
α/°	90
β/°	98.024(3)
γ/°	90
Volume/Å ³	3495.40(18)
Z	4
ρ _{calc} /cm ³	1.295
μ/mm ⁻¹	1.982
F(000)	1424.0
Crystal size/mm ³	0.6 × 0.4 × 0.1
Radiation	CuKα (λ = 1.54184)
2θ range for data collection/°	7.002 to 143.368
Index ranges	-9 ≤ h ≤ 6, -37 ≤ k ≤ 38, -16 ≤ l ≤ 17
Reflections collected	17699
Independent reflections	6615 [R _{int} = 0.0438, R _{sigma} = 0.0378]
Data/restraints/parameters	6615/0/445
Goodness-of-fit on F ²	1.025
Final R indexes [I > 2σ (I)]	R ₁ = 0.0662, wR ₂ = 0.1847
Final R indexes [all data]	R ₁ = 0.0780, wR ₂ = 0.2029
Largest diff. peak/hole / e Å ⁻³	0.49/-0.53

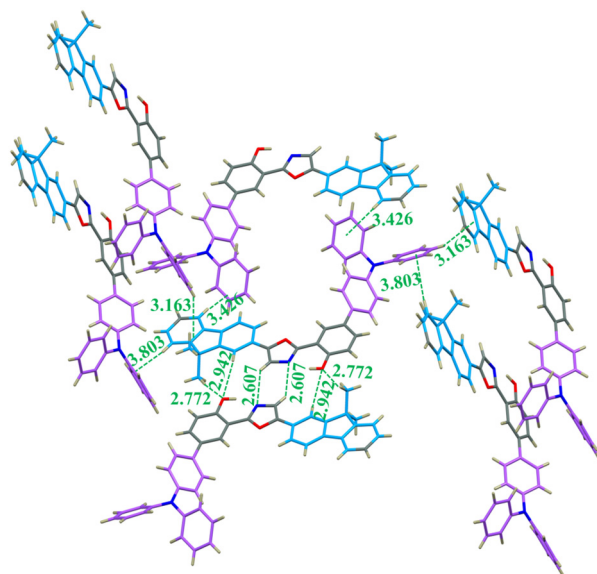


Figure S40. Packing structure of the yellowish-green-emitting single crystal of **6b** (C–H···N 2.607 Å, C–H···O 2.772, 2.942 Å, and C–H··· π 3.163, 3.426, 3.803 Å).

Table S5. Crystal data for white-emitting single crystal of **6b**.

Identification code	Yjs-hq-w6b
Empirical formula	C ₄₂ H ₃₂ N ₂ O ₂
Formula weight	596.69
Temperature/K	150.00(10)
Crystal system	triclinic
Space group	P-1
a/Å	10.5918(4)
b/Å	11.6746(5)
c/Å	13.7260(5)
α /°	103.723(3)
β /°	94.505(3)
γ /°	107.201(4)
Volume/Å ³	1554.74(11)
Z	2
$\rho_{\text{calc}}/\text{cm}^3$	1.275
μ/mm^{-1}	0.611
F(000)	628.0
Crystal size/mm ³	0.6 × 0.4 × 0.2
Radiation	CuK α (λ = 1.54184)
2 θ range for data collection/°	8.242 to 143.78
Index ranges	-13 ≤ h ≤ 13, -14 ≤ k ≤ 14, -14 ≤ l ≤ 16
Reflections collected	16949

Independent reflections	5950 [$R_{\text{int}} = 0.0441$, $R_{\text{sigma}} = 0.0366$]
Data/restraints/parameters	5950/0/418
Goodness-of-fit on F^2	1.024
Final R indexes [$I \geq 2\sigma(I)$]	$R_1 = 0.0568$, $wR_2 = 0.1490$
Final R indexes [all data]	$R_1 = 0.0616$, $wR_2 = 0.1563$
Largest diff. peak/hole / $e \text{ \AA}^{-3}$	0.23/-0.34

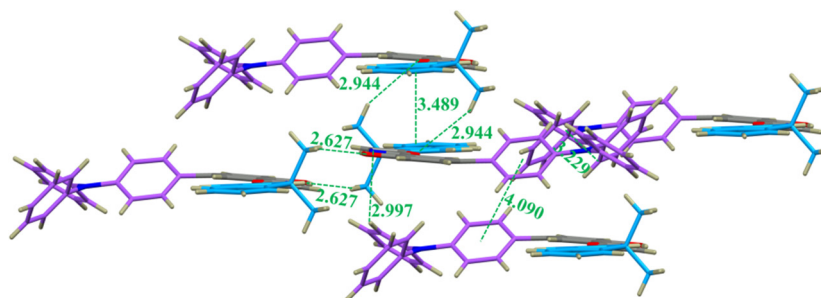


Figure S41. Packing structure of the white-emitting single crystal of **6b** ($\pi \cdots \pi$ 3.229, 3.489, 4.090 Å, C–H \cdots N 2.997 Å, and C–H \cdots O 2.627, 2.944 Å).

VIII. Theoretical calculation

All theoretical calculations were performed using Gaussian 16 package. Frontier molecular orbitals of molecules **6a** and **6b** were obtained by ω B97XD density functional method with basis set 6-311G**. The geometries were fully optimized using density functional theory (DFT) with a polarizable continuum model (PCM) in toluene. The HOMO distributions and LUMO distributions were visualized using Gaussview 5.0 software.

The Gibbs energy of single molecule in solid phase were calculated by DFT method at ω B97XD/6-311G** level. The two layers ONIOM model is constructed from the crystal structure, the central single molecule is regarded as the high layer and calculated by the quantum mechanics (QM) method. The surrounding molecules are treated as the molecular mechanics (MM) part, which is defined as the low layer. The universal force field (UFF) is adopted for the MM part and the electronic embedding is selected in our QM/MM calculations. Geometric structures of central single molecule in ground state (S_0) and the first singlet excited state (S_1) are fully optimized using DFT method and the time-dependent density functional theory (TDDFT)

respectively. In addition, the molecules of the MM part are frozen during the geometry optimizations for S_0 and the S_1 state. The ω B97XD/6-311G** level is used in all the QM calculations.

The magnitudes and angles of the dipole moment in single molecule state were calculated by DFT method at ω B97XD/def2-SVPD level. Geometric structures of single molecule in ground state (S_0) and the first singlet excited state (S_1) are fully optimized using DFT method and TDDFT by ω B97XD density functional method with basis set 6-31G(d), respectively. The geometric structures in solid state are optimized with the two layers ONIOM model from the crystal structure. The dipole moment was visualized using Gaussview 5.0 software.

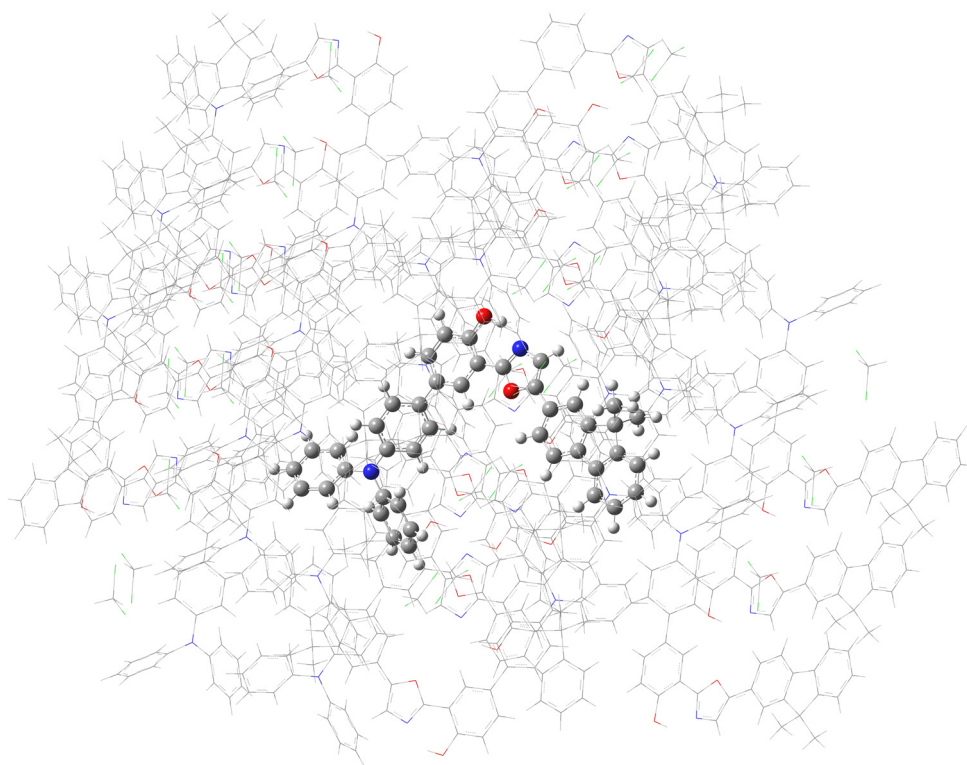


Figure S42. The ONIOM model for yellowish-green-emitting single crystal of **6b** in enol-form S_0 state.

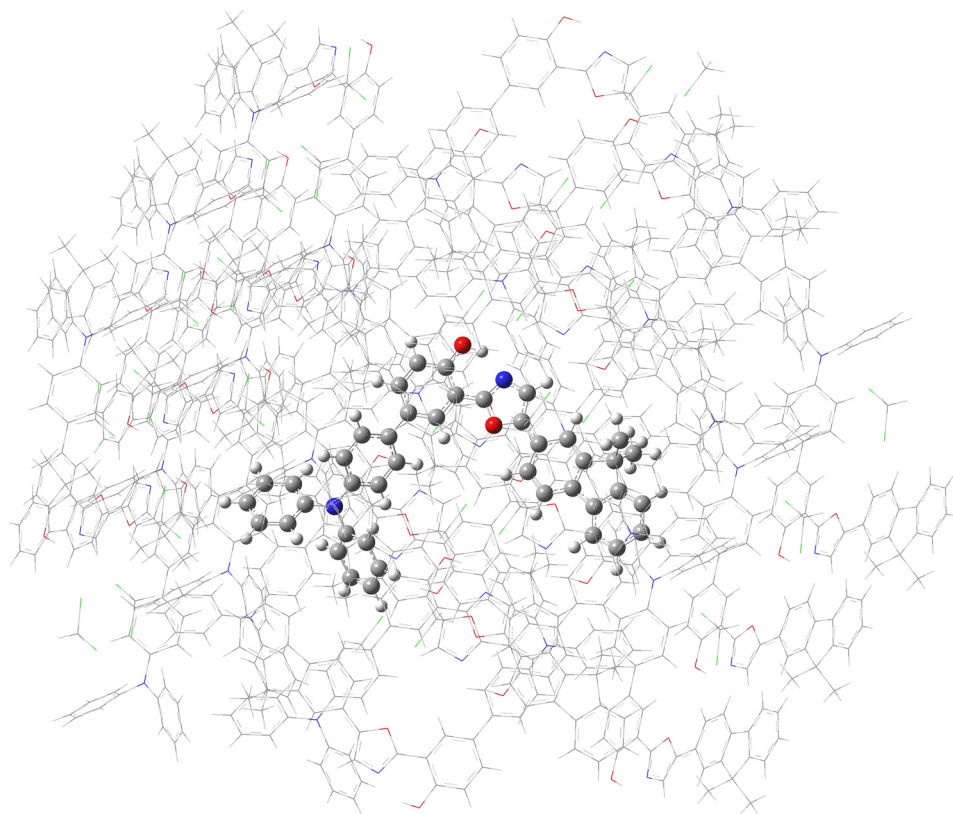


Figure S43. The ONCOM model for yellowish-green-emitting single crystal of **6b** in enol-form S₁ state.

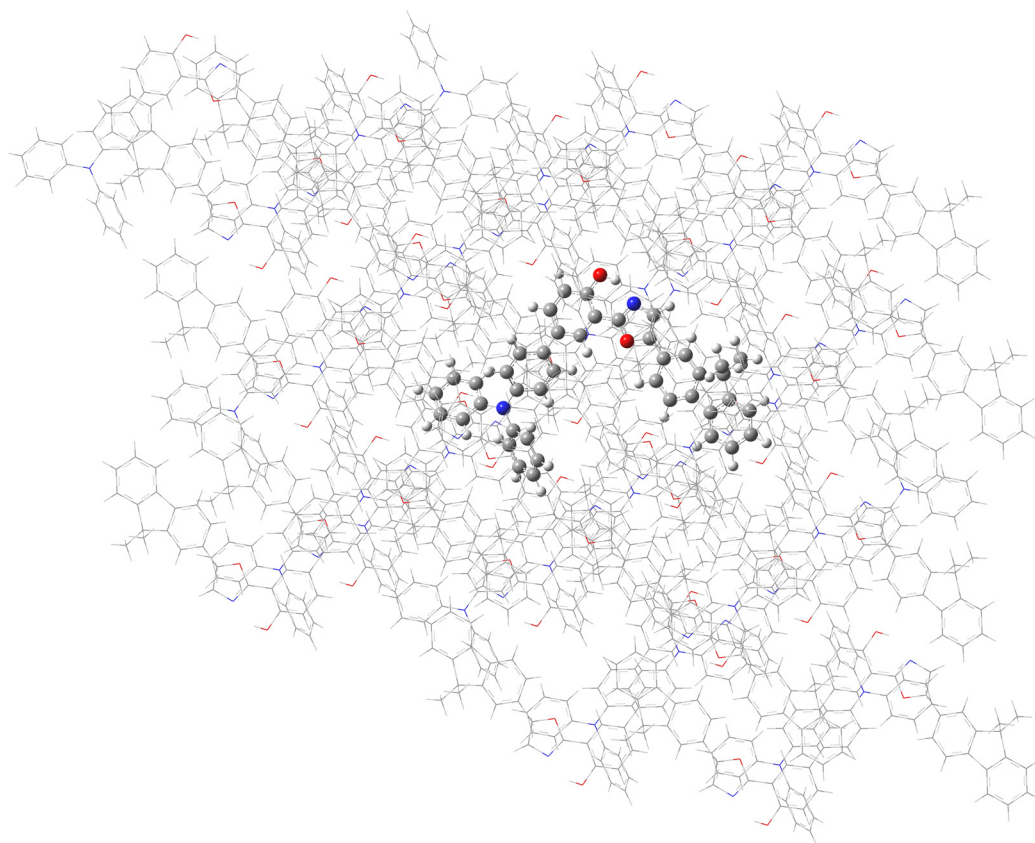


Figure S44. The ONIOM model for white-emitting single crystal of **6b** in enol-form S_0 state.

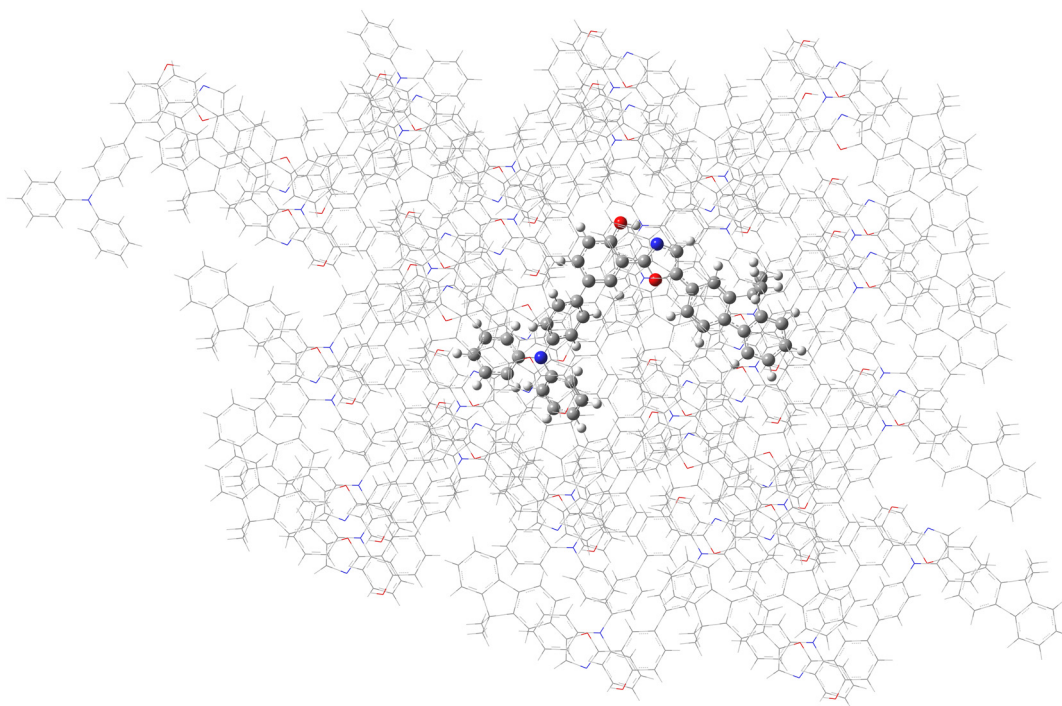


Figure S45. The ONIOM model for white-emitting single crystal of **6b** in enol-form S_1 state.

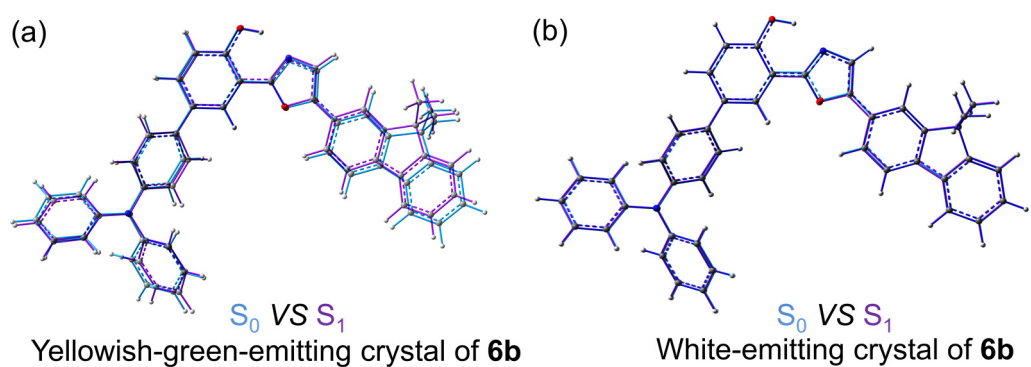


Figure S46. Geometry comparisons of **6b** between S_0 (blue) and S_1 (purple) in (a) yellowish-green-emitting crystals and (b) white-emitting crystals, respectively.

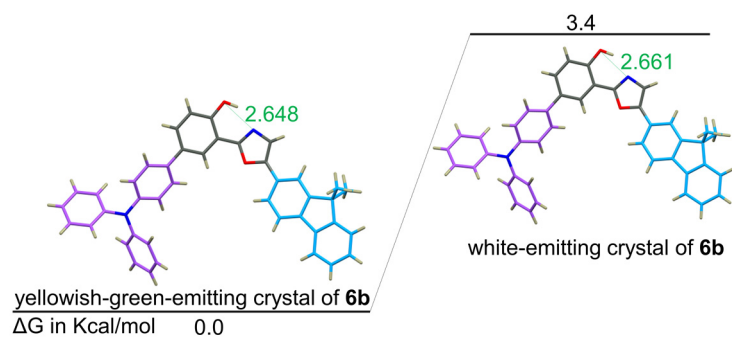


Figure S47. Gibbs energy profile for yellowish-green-emitting single crystal and white-emitting single crystal of **6b**.

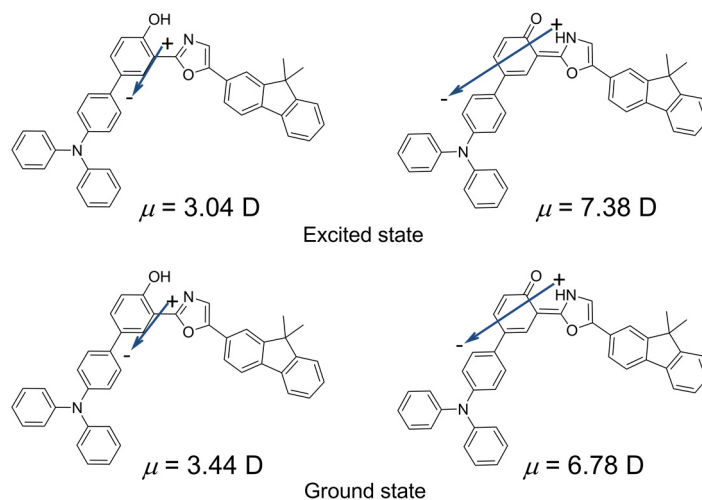


Figure S48. The magnitude and orientation of dipole vectors of the enol and keto forms of **6b** in ground state and excited state, respectively (arrows show components along the x-y plane).

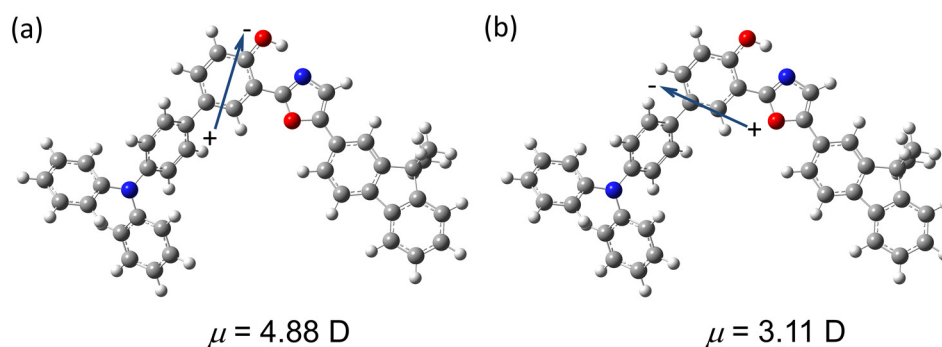
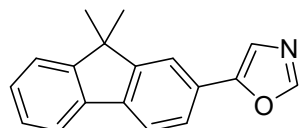


Figure S49. The magnitude and orientation of dipole vectors of (a) the yellowish-green-emitting single crystal and (b) the white-emitting single crystal of **6b** in ground-state enol forms (arrows show components along the x-y plane).

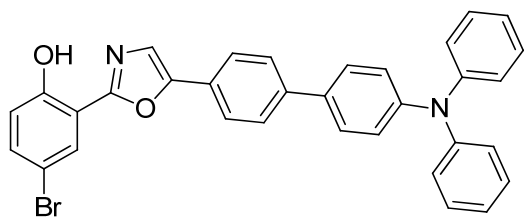
IX. Characterization data of products



5-(9,9-Dimethyl-9H-fluoren-2-yl)oxazole (**2b**)

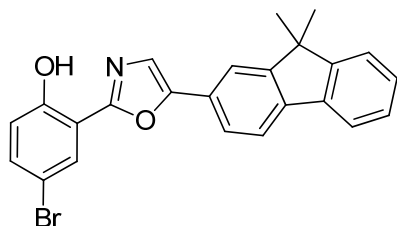
M.p.: 124-126 °C. ^1H NMR (400 MHz, CDCl_3), δ = 7.93 (s, 1H), 7.76-7.73 (m, 2H), 7.71 (s, 1H), 7.66-7.64 (d, J = 8.0 Hz, 1H), 7.46-7.44 (m, 1H), 7.40 (s, 1H), 7.36-7.34 (m, 2H), 1.53 (s, 6H); ^{13}C NMR (100 MHz, CDCl_3), δ = 154.5, 154.0, 152.2, 150.4, 140.0, 138.5,

127.9, 127.3, 126.7, 123.7, 122.8, 121.4, 120.6, 120.4, 118.8, 47.1, 27.2. HRMS (ESI⁺): calcd for C₁₈H₁₆NO [M+H]⁺ 262.1226, found 262.1222.



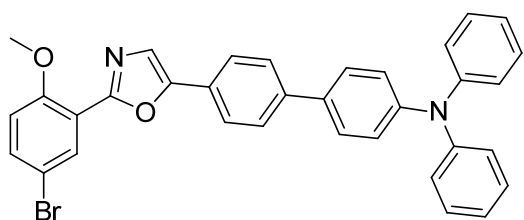
4-Bromo-2-(5-(4'-(diphenylamino)-[1,1'-biphenyl]-4-yl)oxazol-2-yl)phenol (3a)

M.p.: 192-194 °C. ¹H NMR (400 MHz, CDCl₃), δ = 11.33 (s, 1H), 7.81-7.75 (m, 3H), 7.69-7.66 (m, 2H), 7.52-7.50 (m, 2H), 7.45 (s, 1H), 7.31-7.27 (m, 5H), 7.17-7.14 (m, 7H), 7.08-7.04 (t, *J* = 8.0 Hz, 2H); ¹³C NMR (100 MHz, CDCl₃), δ = 160.2, 158.0, 150.4, 147.8, 147.6, 141.3, 133.7, 129.5, 127.7, 127.2, 126.9, 126.0, 125.6, 124.9, 124.7, 123.7, 123.3, 123.0, 121.1, 120.6, 110.3. HRMS (ESI⁺): calcd for C₃₃H₂₄BrN₂O₂ [M+H]⁺ 559.1016, found 559.1018.



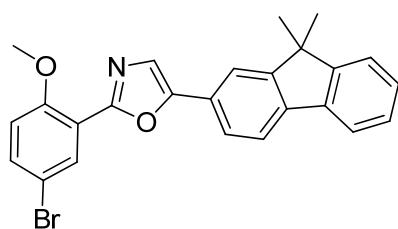
4-Bromo-2-(5-(9,9-dimethyl-9H-fluoren-2-yl)oxazol-2-yl)phenol (3b)

M.p.: 173-175 °C. ¹H NMR (400 MHz, CDCl₃), δ = 11.24 (s, 1H), 8.09 (s, 1H), 7.81-7.70 (m, 4H), 7.49-7.44 (m, 3H), 7.38-7.36 (m, 2H), 6.99 (d, *J* = 8.0 Hz, 1H), 1.58 (s, 6H); ¹³C NMR (100 MHz, CDCl₃), δ = 159.4, 156.5, 154.6, 154.1, 151.4, 140.5, 138.4, 134.9, 128.2, 128.1, 127.4, 126.0, 123.8, 122.9, 121.1, 120.8, 120.5, 119.3, 118.8, 112.9, 111.4, 47.3, 27.3. HRMS (ESI⁺): calcd for C₂₄H₁₉BrNO₂ [M+H]⁺ 432.0594, found 432.0597.



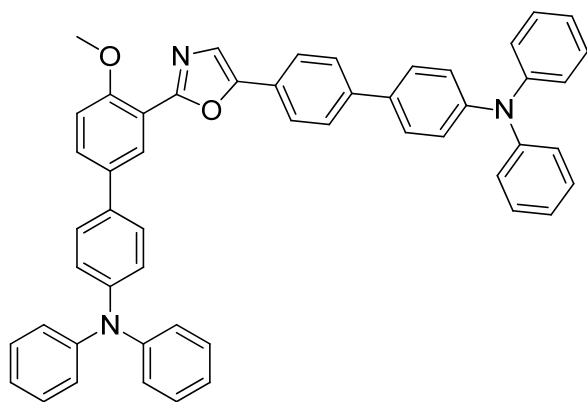
4'-(2-(5-Bromo-2-methoxyphenyl)oxazol-5-yl)-N,N-diphenyl-[1,1'-biphenyl]-4-amine (4a)

M.p.: 175-177 °C. ¹H NMR (400 MHz, CDCl₃), δ = 8.17 (s,1H), 7.77 (d, J = 8.0 Hz, 2H), 7.66 (d, J = 8.0 Hz, 2H), 7.55-7.50 (m, 4H), 7.30-7.27 (m, 4H), 7.16-7.14 (m, 6H), 7.05 (t, J = 8.0 Hz, 2H), 6.95 (d, J = 8.0 Hz, 1H), 4.01 (s, 3H); ¹³C NMR (100 MHz, CDCl₃) δ = 158.0, 156.8, 151.1, 147.72, 147.67, 140.8, 134.2, 134.0, 132.4, 129.5, 127.7, 127.1, 126.3, 124.9, 124.7, 123.8, 123.6, 123.3, 118.3, 113.9, 113.0, 56.6. HRMS (ESI⁺): calcd for C₃₄H₂₆BrN₂O₂ [M+H]⁺ 573.1172, found 573.1175.



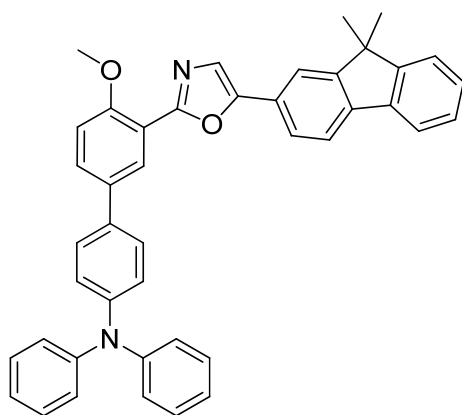
2-(5-Bromo-2-methoxyphenyl)-5-(9,9-dimethyl-9H-fluoren-2-yl)oxazole (4b)

M.p.: 163-165 °C. ¹H NMR (400 MHz, CDCl₃), δ = 8.14 (s,1H), 7.62-7.56 (m, 6H), 7.54-7.51 (m, 2H), 7.15-7.12 (m, 1H), 6.94 (d, J = 8.0 Hz, 1H), 3.99 (s, 3H), 1.29 (s, 6H); ¹³C NMR (100 MHz, CDCl₃) δ = 158.4, 156.8, 151.0, 150.3, 139.2, 137.2, 134.4, 133.6, 132.5, 132.3, 127.7, 126.9, 125.9, 124.1, 122.6, 122.3, 118.1, 113.9, 112.9, 110.1, 92.2, 56.5, 34.7, 31.3. HRMS (ESI⁺): calcd for C₂₅H₂₁BrNO₂ [M+H]⁺ 446.0750, found 446.0748.



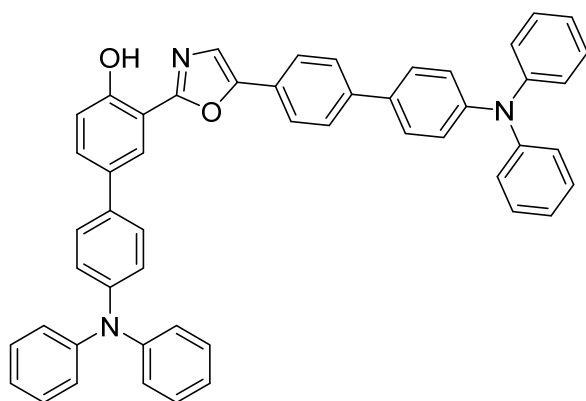
3'-(5-(4'-(Diphenylamino)-[1,1'-biphenyl]-4-yl)oxazol-2-yl)-4'-methoxy-N,N-diphenyl-[1,1'-biphenyl]-4-amine (5a)

M.p.: 240-242 °C. ^1H NMR (400 MHz, CDCl_3), δ = 8.26 (s, 1H), 7.78 (d, J = 8.0 Hz, 2H), 7.66-7.63 (m, 3H), 7.55-7.50 (m, 5H), 7.30-7.28 (m, 6H), 7.19-7.12 (m, 15H), 7.07-7.02 (m, 4H), 4.06 (s, 3H); ^{13}C NMR (100 MHz, CDCl_3), δ = 159.5, 156.9, 150.7, 147.8, 147.7, 147.2, 140.6, 134.1, 133.5, 129.8, 129.5, 129.2, 128.4, 128.2, 127.7, 127.6, 127.1, 126.6, 125.4, 124.8, 124.7, 124.5, 124.2, 123.8, 123.6, 123.2, 123.0, 116.7, 112.6, 56.5. HRMS (ESI⁺): calcd for $\text{C}_{52}\text{H}_{40}\text{N}_3\text{O}_2$ $[\text{M}+\text{H}]^+$ 738.3115, found 738.3112.



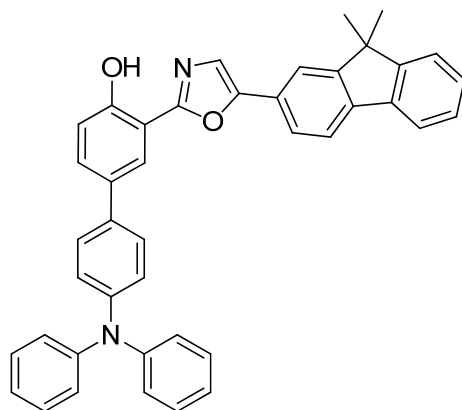
3'-(5-(9,9-Dimethyl-9H-fluoren-2-yl)oxazol-2-yl)-4'-methoxy-N,N-diphenyl-[1,1'-biphenyl]-4-amine (5b)

M.p.: 237-239 °C. ^1H NMR (400 MHz, CDCl_3), δ = 8.27 (s, 1H), 7.80-7.73 (m, 4H), 7.67-7.64 (m, 1H), 7.57-7.52 (m, 3H), 7.47-7.45 (m, 1H), 7.36-7.34 (m, 2H), 7.28 (t, J = 8.0 Hz, 4H), 7.19-7.13 (m, 7H), 7.06-7.03 (m, 2H), 4.06 (s, 3H), 1.52 (s, 6H); ^{13}C NMR (100 MHz, CDCl_3), δ = 159.4, 156.9, 154.4, 154.0, 151.5, 147.8, 147.2, 139.7, 138.7, 134.2, 133.5, 129.8, 129.4, 128.2, 127.8, 127.7, 127.3, 127.1, 124.5, 124.2, 123.6, 123.4, 123.1, 122.8, 120.6, 120.3, 118.6, 116.9, 112.6, 56.5, 47.1, 27.3. HRMS (ESI⁺): calcd for $\text{C}_{43}\text{H}_{35}\text{N}_2\text{O}_2$ $[\text{M}+\text{H}]^+$ 611.2693, found 611.2696.



4'-(Diphenylamino)-3-(5-(4'-(diphenylamino)-[1,1'-biphenyl]-4-yl)oxazol-2-yl)-[1,1'-biphenyl]-4-ol (6a)

M.p.: 231-233 °C. ^1H NMR (400 MHz, CDCl_3), δ = 11.21 (s, 1H), 8.12 (s, 1H), 7.80-7.78 (m, 2H), 7.68-7.66 (m, 2H), 7.60-7.57 (m, 1H), 7.53-7.50 (m, 4H), 7.47 (s, 1H), 7.31-7.27 (m, 8H), 7.19-7.14 (m, 13H), 7.08-7.03 (m, 4H); ^{13}C NMR (100 MHz, CDCl_3), δ = 160.9, 156.7, 150.3, 147.8, 147.6, 147.0, 141.1, 134.5, 133.8, 132.5, 130.9, 129.5, 129.4, 127.7, 127.6, 127.2, 125.8, 124.9, 124.7, 124.4, 124.3, 123.8, 123.7, 123.3, 123.0, 121.2, 117.7, 111.4. HRMS (ESI⁺): calcd for $\text{C}_{51}\text{H}_{38}\text{N}_3\text{O}_2$ [M+H]⁺ 724.2959, found 724.2955.



3-(5-(9,9-Dimethyl-9H-fluoren-2-yl)oxazol-2-yl)-4'-(diphenylamino)-[1,1'-biphenyl]-4-ol (6b)

M.p.: 230-232 °C. ^1H NMR (400 MHz, CDCl_3), δ = 11.30 (s, 1H), 8.15 (s, 1H), 7.81-7.73 (m, 4H), 7.60 (d, J = 8.0 Hz, 1H), 7.54-7.46 (m, 4H), 7.38-7.36 (m, 2H), 7.29 (t, J = 8.0 Hz, 4H), 7.21-7.15 (m, 7H), 7.05 (t, J = 8.0 Hz, 2H), 1.57 (s, 6H); ^{13}C NMR (100 MHz, CDCl_3), δ = 160.8, 156.7, 154.6, 154.0, 151.0, 147.8, 147.1, 140.2, 138.5, 134.6, 132.5, 130.9, 129.5, 128.0, 127.7, 127.3, 126.3, 124.5, 124.3, 123.7, 123.0, 122.9, 121.1, 120.7, 120.4, 118.7, 117.8, 111.4, 47.2, 27.3. HRMS (ESI⁺): calcd for $\text{C}_{42}\text{H}_{33}\text{N}_2\text{O}_2$ [M+H]⁺ 597.2537, found 597.2537.

X. References

- 1 B. Li, J. Lan, D. Wu and J. You, *Angew. Chem. Int. Ed.* 2015, **54**, 14008.
- 2 N. A. Strotman, H. R. Chobanian, Y. Guo, J. He and J. E. Wilson, *Org. Lett.* 2010, **12**, 3578.
- 3 Z. Zhang, Y.-A. Chen, W.-Y. Hung, W.-F. Tang, Y.-H. Hsu, C.-L. Chen, F.-Y. Meng and P.-T. Chou, *Chem. Mater.* 2016, **28**, 8815.

XI. Copies of ^1H and ^{13}C NMR spectra

